International Journal of GEOMATE, Jan., 2023, Vol.24, Issue 101, pp.110-117
ISSN: 2186-2982 (P), 2186-2990 (O), Japan, DOI: https://doi.org/10.21660/2023.101.3721
Geotechnique, Construction Materials and Environment

EFFECT OF BOTTOM WALL FRICTION ON THE TRANSITION OF DEVELOPMENTAL STAGES OF GRAVITY CURRENT

* Jinichi Koue [1]

[1] Graduate school of Maritime Sciences, Kobe University, Japan

*Corresponding Author, Received: 27 Nov. 2022, Revised: 19 Dec. 2022, Accepted: 10 Jan. 2023

ABSTRACT: In experiments of locked-exchange flow, the flow structure at the head of the gravity current was examined. In a rectangular channel, a finite volume of fluid was instantaneously released into another fluid of slightly different density. By comparing the effect of the bottom shape, how the bottom wall friction influences transition to the stage of the developing gravity current was investigated. The movement of the position of the head of the gravity current was visualized by a digital video camera. As a result, it was found that when no disturbance from behind came to the head during the viscous stage, the front decelerated with the time to the power of 1/2 even in the case of existence of effect of bottom wall. The transition time from the initial stage to the viscous stage was shown to vary with the Reynolds number even in the change of shape in the bottom. The three-dimensional instability of the flow contributed to the mixing process through the head and the density interfaced behind it, which also affected the head velocity.

Keywords: Gravity current; Head edge; Transition time; The three-dimensional instability.

1. INTRODUCTION

Gravity currents are flows caused by temperature and density differences. There are a variety of processes that cause gravity currents, from natural causes such as ocean currents, tides, freshwater inflows, coastal upwelling, and turbulent mudflows on the seafloor [1, 2], as well as those caused by human factors such as thermal discharge from thermal power plants and oil spills caused by tankers in maritime accidents [3]. Gravity currents have density boundary surfaces, and when gravity currents pass through them, the density boundary surfaces prevent vertical mass transport, causing the negative effects such as a lack of nutrients and oxygen in the lower layers divided by the boundary surface layers [4, 5]. Therefore, predicting when, where, and how the head of gravity current will form is extremely important for the marine environment.

A basic model for studying the behavior of the head location of gravity currents is the lock-exchange problem. In the lock-exchange problem, a tank is kept horizontal, the lock gate is placed vertically in the tank, and two fluids with different densities are added to both sides of the tank with the lock gate as a boundary. Various studies have been conducted on this lock-exchange problem about the gravity currents traveling along a horizontal, flat surface, flowing down a slanted bottom [6-13], and flowing along the effects of bottom roughness elements [14].

Given the influence of the wall of the water tank, the released fluid spreads at a constant velocity at the initial stage, then slows down so that the front velocity decreases with time to the power of 2/3 [15] in the self-similar regime. When no disturbance from behind comes to the head, the current that has begun to be dominated by viscosity slows down further in the viscous stage dominated by viscosity, the front decelerates with the time to the power of 1/5. Each developmental stage has previously been replicated with the water tank and displayed by the energy conversion in the box model [16].

In the case of the gravity current with a larger initial length than usual and no effect of reflection from the side wall generated behind the gravity current, the head position transitions from the initial stage, which is proportional to the time, to the viscous stage, which is proportional to the time to the power of 1/2.

The head position varies not only with density difference and water depth, but also with its developmental stage. However, the effect of the bottom shape of wall friction on the head position of gravity flow has not been clarified yet, although studies have been conducted on the lock-exchange problem under conditions where the wall friction of the tank is unaffected.

In this study, the effects of the shape of bottom wall friction on the head position of the gravity current in the developmental stage were investigated by calculating the position of the gravity current by the box model and conducting the experiment by changing the bottom wall friction in the lock-exchange problem.

2. RESEARCH SIGNIFICANCE

Gravity currents are commonly generated in lakes, estuaries, and oceans with a specific bed slope. Stratification exists in these environments because of uneven temperature distribution and salinity diffusion. Furthermore, the propagation and dynamics of gravity currents influences the vegetation zones such as reeds and mangroves in the near shore. In order to understand how stratified environments and vegetation zones are influenced is to analyze the propagation of gravity currents. The results of this study can also provide a scientific basis for the construction of marine environments and disaster prevention and mitigation on the coasts.

3. METHODOLOGY

The theoretical, experimental, and numerical investigation of gravity current propagation in a long channel of length L and water depth H was conducted. Fig.1 depicts a water tank with L=4000mm length and D=60mm depth. The lock gate was placed from the edge of the water tank to the position of distance $\boldsymbol{x_0} = \boldsymbol{L/2}$, the fluid with the density of $\boldsymbol{\rho_0}$ was placed in one area partitioned by the lock gate, and the fluid with the density of $\boldsymbol{\rho_0 + \Delta\rho}$ was placed in the other. As for the density difference of the fluid, the case of several percent salt water was used to do this experiment. The behavior and structure of the head of the gravity current after the lock gate was opened was examined.

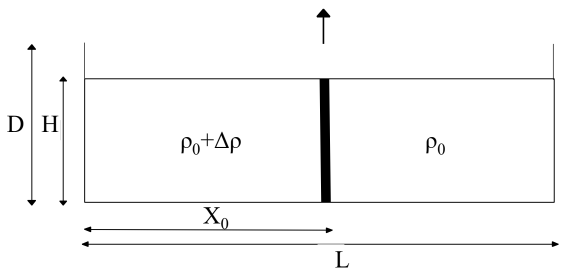

Fig. 1 A schematic diagram of lock-exchange flow

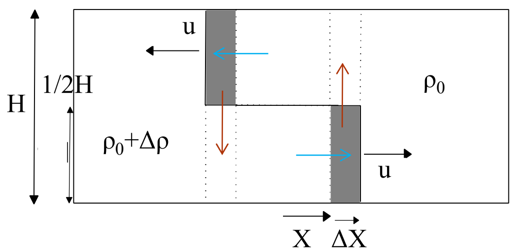

Fig. 2 (a) Initial stage of gravity current

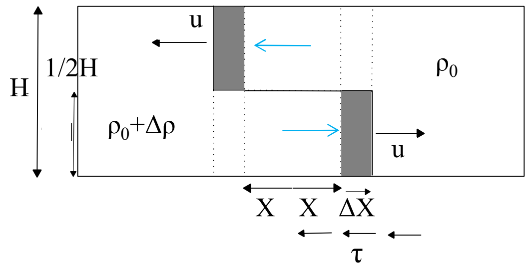

Fig. 2 (b) Viscous stage of the gravity current

3.1 Box Model

Fig. 2 (a) depicts the initial stage after the lock gate is opened. The fluid exchange occurred in relation to the symmetry position of the lock gate, the height of the gravity current became half of its initial value, and it progressed. The amount of energy change between the state after the lock gate is opened and the state where the head of the gravity current advances distance x is taken into account. The amount of the change in potential energy, **ΔP**, by the gravity current is given by

$$\mathbf{\Delta P = -\frac{1}{4}\Delta\rho\Delta x \cdot gH^2} \tag{1}$$

where Δρ is the difference in density, Δx is the difference in distance, g is the gravitational acceleration, and H is the water depth.

It is equal to the potential energy when a heavy fluid falls only half of the initial height and is exchanged for a light fluid.

The change in kinetic energy of the head, ΔK, can be expressed as

$$\mathbf{\Delta K = \rho_0 \cdot \Delta x \cdot H \cdot v^2} \tag{2}$$

where ρ is the density of fluid in the head, and v is the characteristic velocity.

Assuming that dynamic energy is conserved and that all decreasing potential energy is used to generate kinetic energy,

$$\mathbf{\Delta P + \Delta K = 0} \tag{3}$$

therefore, the front velocity is given by

$$\mathbf{v = \frac{1}{2}\sqrt{\frac{\Delta\rho}{\rho_0}gH}} \tag{4}$$

The viscous stage is depicted in Fig. 2(b), where friction is created between the progressing fluid and the bottom of the wall. When a rectangular area of

fluid distance of x in length moves the distance of Δx along the bottom of the wall,
the change in dissipative energy, ΔD, can be written in the form of

$$\Delta D = \tau x \Delta x \quad (5)$$

where shearing stress τ is regarded to be proportional to the velocity,

$$\tau = \mu \frac{1}{H}\frac{dx}{dt} \quad (6)$$

and μ denotes the viscosity coefficient of the fluid. If the dissipative energy is entirely due to a decrease in potential energy, the distance moved x is given by

$$x = \sqrt{\frac{1}{2}}\sqrt{\frac{\Delta\rho}{\mu} g H^3 t} \quad (7)$$

When the viscosity on the wall becomes dominant, the front velocity decreases as the distance moved is proportional to the time to the power of 1/2.

The gravity current progresses due to the potential energy of the density difference, and in terms of energy conversion, gravity current development stages can be divided into two stages: the initial stage and the viscous stage.

3.2 Experimental Condition

In this study, the experiment was conducted with the lock-exchange problem.

The water tank was an acrylic and aluminum tank of length L=4000mm, width B=113mm, and depth H=60mm. The length of the water tank was large enough to avoid the influence of reflected waves. A guide was attached to the center of the tank so that an acrylic partition plate could slide vertically up and down. At this time, the partition was carefully installed without any gaps to prevent water leakage. To prevent water leakage, grease was applied to the partition plate during the experiment.

The lock gate was placed at the middle of the water tank, the fluid with the density of ρ_0 was placed in one area partitioned by the lock gate, and the fluid with the density of $\rho_0 + \Delta\rho$ was placed in the other. The less dense fluid ρ_0 was fresh water and the denser fluid $\rho_0 + \Delta\rho$ was a solution of water and sodium chloride with red dye. A gravimeter and refractometer were used to measure the density ratio.

A digital video camera was used to measure and visualize the position of the head of the gravity current. The images were captured by a computer and the time at each 50 mm distance from the lock gate was recorded. The water depth H was set to 25mm, and the density differences between the two fluids were 1%, 2%, and 4%, respectively. The Reynolds numbers were 1086, 1536, and 2348, in that order.

In order to analyze how the flow structure of gravity flow due to the effect of wall viscosity fluctuates, the shape of the bottom wall surface was changed. In changing the shape of the wall surface, vinyl sheets were used.

The lengths of the vinyl chloride sheets shown in Fig. 3 were $d_1 = 1.45mm$, $d_2 = 0.8mm$, $x_1 = 1.9mm$, and $x_2 = 3.15mm$, respectively. One of the vinyl chloride sheets were painted white so that the motion of gravity current could be easily observed. As shown in Fig. 4, two patterns of sheets were used to conduct the experiment, one with the unevenness in Fig. 3 parallel to the direction of gravity current (Horizontal friction), and the other with the unevenness perpendicular to the direction of gravity current (Vertical friction).

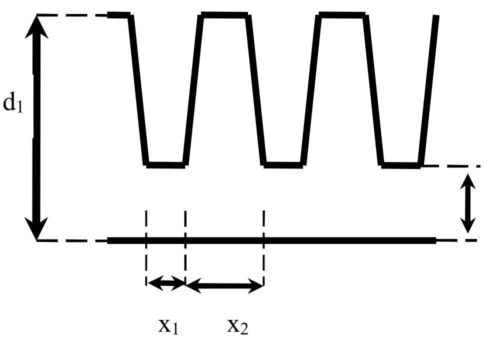

Fig.3 Cross-sectional shape of vinyl chloride sheet

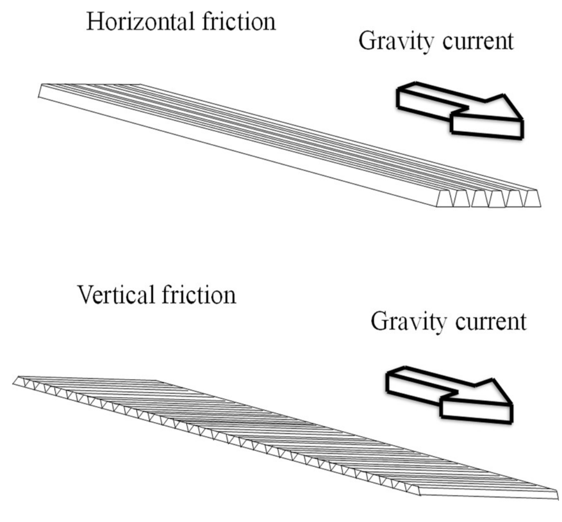

Fig.4 Type of vinyl chloride sheet laid on the bottom

4. RESULT AND DISCUSSIONS

4.1 Effect of Bottom Shape on the Head of Velocity Variations of the Gravity Current

The experimental values were non-dimensionalized with the representative length as the water depth and the representative time as the time.

Fig. 5 (a) ~ (c) show the change in the distance traveled by the head of the gravity current over time for the cases of 1%, 2%, and 4% density difference and 25 mm water depth. The larger the density difference, the faster the gravity current reached the side wall, indicating that the larger the density difference, the faster the gravity current advanced. This was consistent with equation (4). Immediately after the lock gate was opened, the gravity current proceeded at a constant velocity in each density difference, and it was observed that there was a difference in time for reaching the side wall depending on the shape of the wall friction. The horizontal friction and the vertical friction type reached the wall in this order for all density differences, although only slightly, suggesting that the effect of the wall shape on the gravity flow varied.

Next, Fig. 6 (a) ~ (c) show the results of the logarithmic graph of the data on the time variation of the head position of the same gravity current as in Fig. 5. It was observed that the head position transitioned from the initial stage proportional to the time to the viscous stage proportional to the time to the power of 1/2, even when there were horizontal and vertical frictions. The reason why the viscous stage with a slope of 1/2 was not observed in the graph with a density difference of 4% was that the gravity current reached the side wall just after reaching the transition point, and thus the slope did not reach 1/2.

In each density difference, the transition point was delayed in the order of bottom friction, horizontal friction and the vertical friction. This difference in transition time was the reason for the earlier transition to the viscous stage in the same order in Fig. 6.

Fig.7 (a) shows the side snapshot of the head of the gravity current in the case of 1% density difference in the bottom friction case. After the lock gate was opened, the density interface collapsed and fluid exchange began symmetrically. As the density interface near the lock gate approached horizontally, the interface at the head extended vertically and the whole area became box-shaped. As the flow progressed further, the head edge collapsed at the corner and became streamlined, and the density interface behind it rolled up. This indicated that the fluids in the upper and lower layers started to move in opposite directions and the velocity difference at the interface increased, indicating the appearance of Kelvin-Helmholtz instability. In the roll formed by the roll-up of the interface, the distance between the density contours gradually became wider, indicating that mixing of the upper and lower fluids had occurred.

Fig.7 (b) ~ (d) show the snapshot of the head of the gravity current in the case of 1% density difference in bottom friction case, horizontal friction case, and vertical friction case. In the bottom friction case, immediately after the opening of the lock gate, the head of the gravity current deformed in a lateral direction all at once, forming a series of many arc-shaped peaks that extend forward. The size of the arcs varied, but the first overhanging arcs gradually merged into a larger arc by taking in the surrounding arcs. The number of arcs in the horizontal direction decreased, and after several large arcs appeared in the width direction of the tank, multiple smaller arcs emerged from within the arcs again.

These experimental results showed that the head edge of the gravity flow lead to three-dimensional instability immediately after the onset and transitions to a three-dimensional flow. This transition occurred simultaneously with a specific scale in the lateral direction, and the scale was small compared to the width of the tank. This instability was caused not by external factors such as initial disturbance or the effect of side walls, but by the structure of the head. In the horizontal friction case, compared with the case of bottom friction, the first overhanging arc did not take in the surrounding arc and flew along the radial channel type without changing their shape. In vertical friction case, compared with the case of the bottom friction, the first overhanging arc took in the surrounding arc and the head of the gravity current flew more slowly than the one in case of the bottom friction.

The three-dimensional instability caused the head to form a wavy frontline composed of masses of heavy fluid moving ahead as a mountain-valley structure. Because each of the masses fell down laterally as well as forward, it spread out in all directions to form an arc front. Some of them grew in size by running over other masses. The enlarged masses were once again unstable, and some smaller-scale arcs appeared in this.

As a result, the frontline of the gravity current consisted of the boundaries of these masses of varying scales, which were frequently superimposed on each other. It was independent of the instability of the wall boundary layer. The three-dimensional flow structure could make a significant contribution to the mixing process across the density interface behind and in front of the head, which affected the head velocity of the gravity current.

The change in the structure of the head of the gravity current when the shape of the bottom was varied affected the head velocity. When the three-dimensional instability became more pronounced due to the bottom shape, the three-dimensional spreading of the gravity current slowed down the velocity in the direction of travel due to the effect of velocities other than in the direction of travel of each other. The effect of the bottom friction and the turbulence caused by the bottom shape could have an effect of the head velocities. It is important to consider the effect of bottom shape in gravity current over the walls of the seafloor, lake bottoms, and any offshore structure in order to understand nutrient transport conditions.

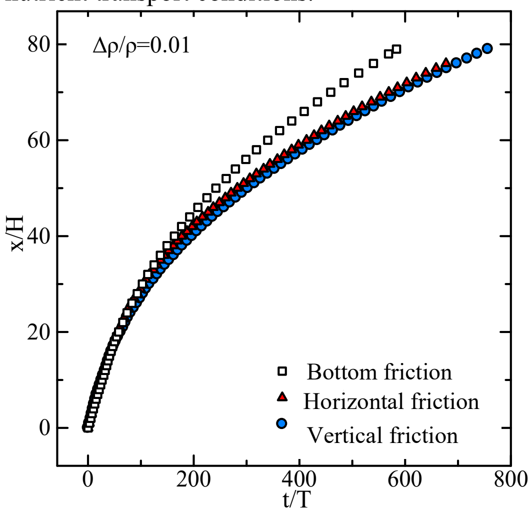

Fig.5 (a) The position of the head of the gravity current over time in the case of 1% density difference

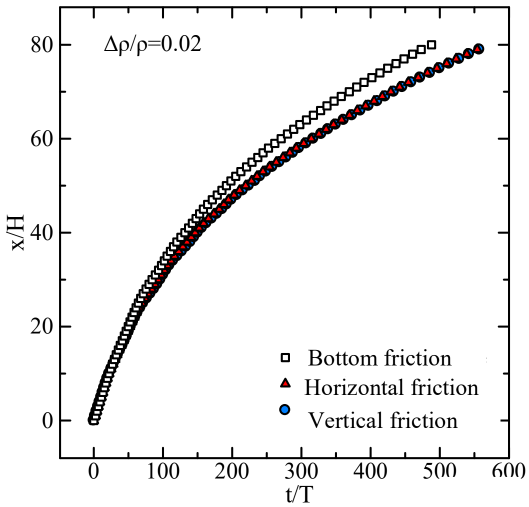

Fig.5 (b) The position of the head of the gravity current over time in the case of 2% density difference

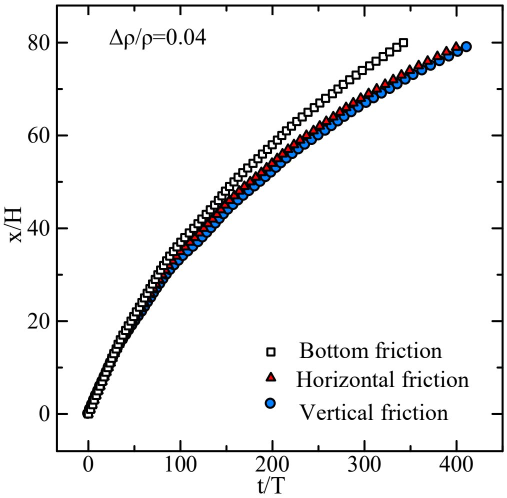

Fig.5 (c) The position of the head of the gravity current over time in the case of 4% density difference

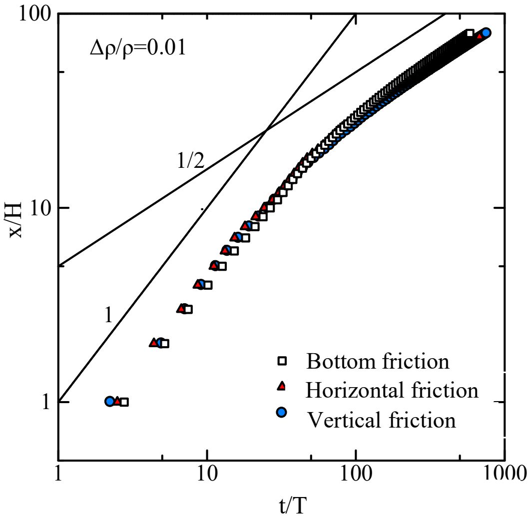

Fig.6 (a) The position of the head of the gravity current over time in the case of 1% density difference in the logarithmic scale

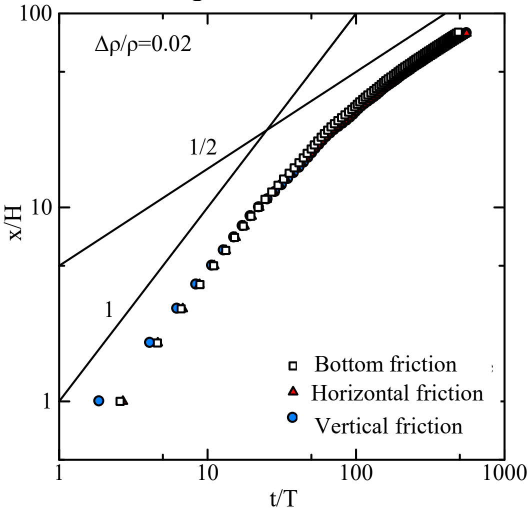

Fig.6 (b) The position of the head of the gravity current over time in the case of 2 % density difference in the logarithmic scale

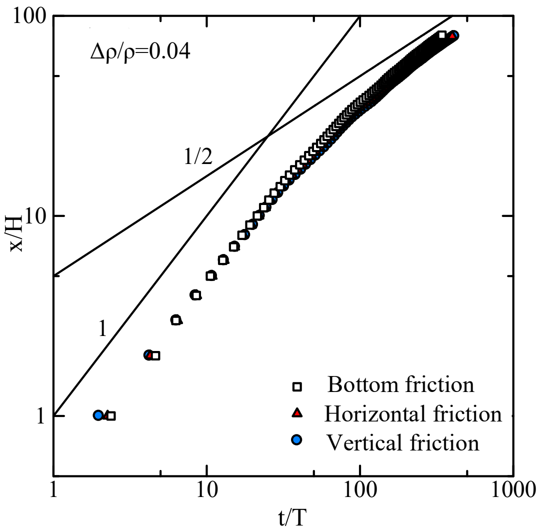

Fig.6 (c) The position of the head of the gravity current over time in the case of 4% density difference in the logarithmic scale

Fig.7 (a) The side snapshot of the head of the gravity current in the case of 1% density difference in bottom friction case.

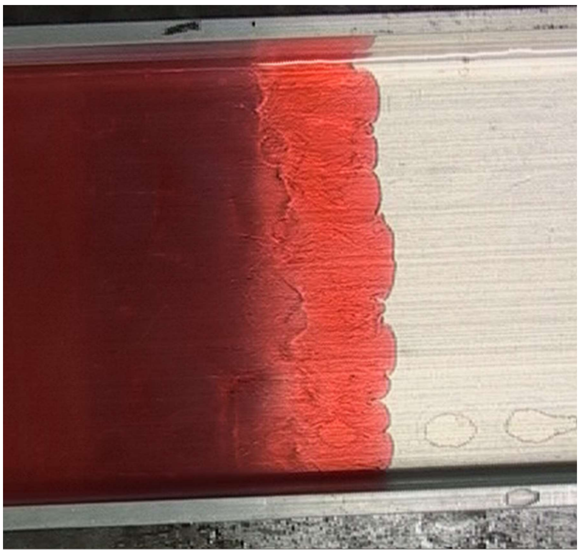

Fig.7 (b) The above snapshot of the head of the gravity current in the case of 1% density difference in bottom friction case.

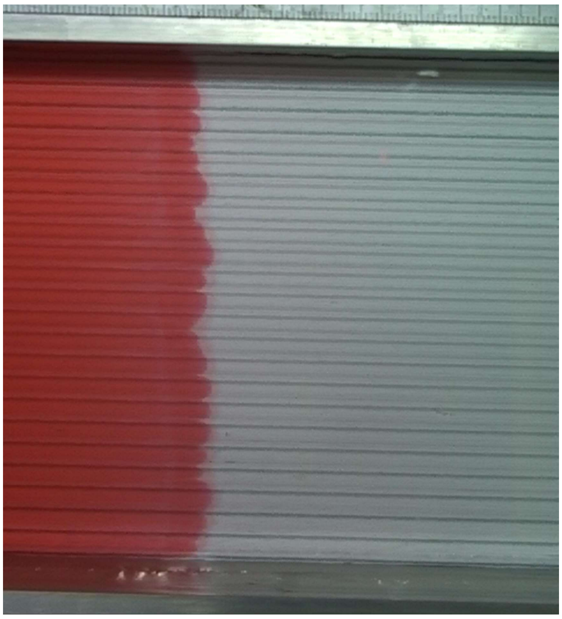

Fig.7 (c) The above snapshot of the head of the gravity current in the case of 1% density difference in horizontal friction case.

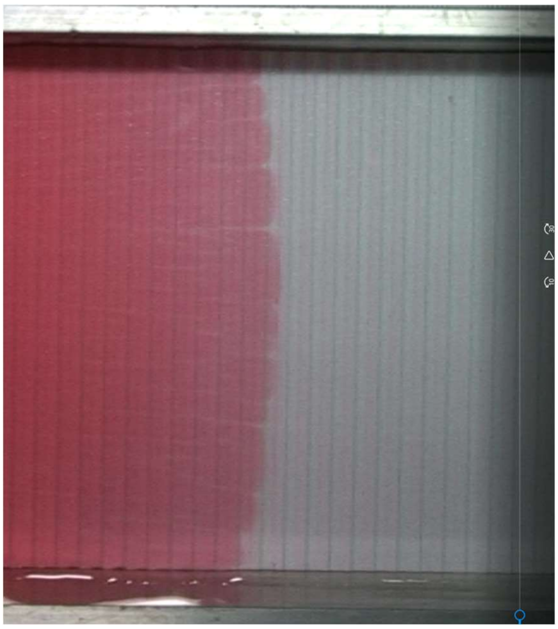

Fig.7 (d) The above snapshot of the head of the gravity current in the case of 1% density difference in vertical friction case.

4.2 Relation Between Time of the Transition Point and the Change in Reynolds Number

The relation between dimensionless time of the transition point and the change in Reynolds number was examined. The transition point was defined as the intersection of a straight line at the initial stage, where the front velocity advanced at a constant velocity, and the one at the viscous stage, where the distance moved was proportional to the time to the power of 1/2, just as shown in Fig. 8 as reference. Moreover, each straight line was obtained by the least-squares method in the cases of Reynolds number 50,200,500,1086,1536,1900, and 2348.

The dimensionless time of the transition point from the first stage to the viscous stage was proportional to the Reynolds number, from the graph of Fig. 9 as reference.

Fig.10 shows the relationship between change in Reynolds number and dimensionless time at transition point of the gravity current in each case of the friction type in this experiment.

In the bottom friction case, the horizontal friction case, and the vertical friction case, the dimensionless time of the transition point from the first stage to the viscous stage was proportional to the Reynolds number in each case.

In the horizontal and vertical friction cases, the transition time was found to be earlier than in the bottom friction case, depending on the shape of the friction. Furthermore, in the case of vertical friction, more three-dimensional instability occurred at the head edge of the gravity current than in the case of horizontal friction, and the velocity of the gravity current slowed down earlier and the time to the viscous stage was earlier.

Changing the head of the gravity current by varying the shape of the bottom is important for controlling gravity flow behavior, and these results are useful for predicting the ambient flow environment that can be drawn in by the gravity flow.

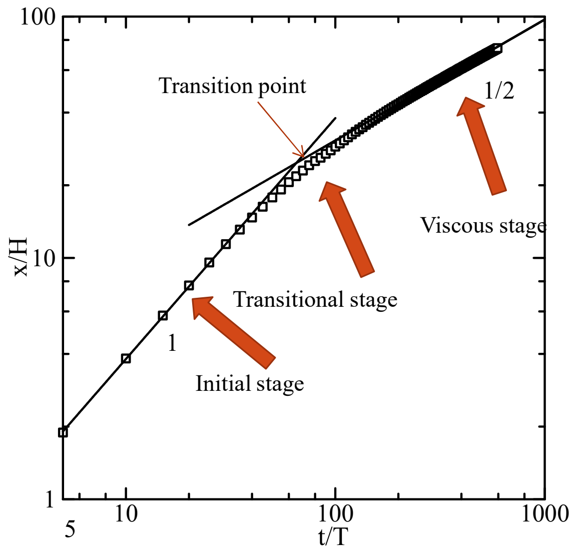

Fig. 8 The position of the head of the gravity current with time in the simulation in logarithmic scale (Re=1086)

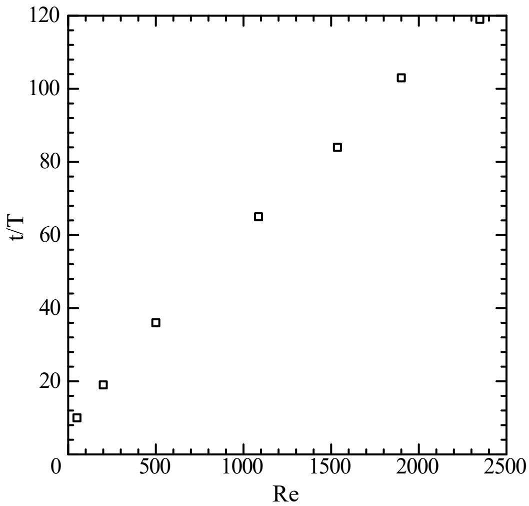

Fig. 9 The relationship between change in Reynolds number and dimensionless time at transition point in the simulation

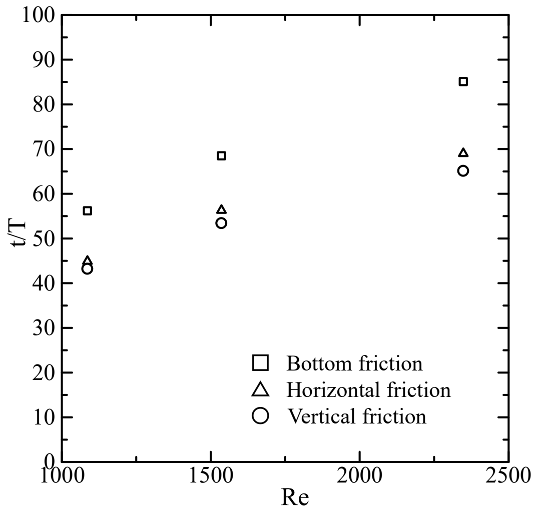

Fig.10 The relationship between change in Reynolds number and dimensionless time at transition point

5. CONCLUSIONS

The dynamic structure of the head of the gravity current was investigated by the experiment and the box model in the range of the Reynolds number 1000-2500. The transition of the developmental stage of the gravity current without the influence of the wall of the water tank was examined by applying the box model.

1) The box model results showed that the front advanced at a constant velocity during the initial stage and decelerated with a time to power of 1/2 during the viscous stage.

2) At the initial stage, the gravity current caused a mass concentration at the head. The gravity current decelerated due to the influence of viscosity as the mass of the head concentration decreased. At the viscous stage, mass concentration at the head was no longer present.

3) The transition from the initial stage to the viscous stage occurred at the time, which was proportional to the Reynolds number even in each friction case.
4) The three-dimensional instability at the head edge of the gravity current extended laterally and deformed three-dimensionally.

At the front, the heavy flow mass at the head edge collapsed in the lateral direction as well as the direction of motion, and spread radially from the head edge. The head edge of the spreading mass became unstable again, and several head sections with small arc-shaped head edges emerged from it. The head edge of the gravity current consisted of multiple arcs spreading in this manner, and these arcs had an overlapping structure. In case of horizontal friction, this three-dimensional instability was large, and many of the wave arc overlapped each other, slowing down the head velocity. In case of vertical friction, there were also more friction areas against the fluid than in the case of bottom friction alone, resulting in slower head velocities. The three-dimensional instability of the flow contributed to the mixing process through the head and the density interfaced behind it, which affected the head velocity.

Gravity currents flowing through stratified surroundings generate internal waves and bores, which play an important role in mass transfer of nutrients. It can contribute to fisheries by helping to determine the location of the density sea surface where there are abundant nutrients in stratified water. In disaster prevention, controlling the shape of the head edge of gravity flow in the change of bottom friction and reducing the head edge velocity could prevent the flow of tsunamis in case of earthquakes and oil leaks due to ship collisions.

6. REFERENCES

[1] Simpson J. E., Gravity Currents: in the Environment and the Laboratory ,2nd ed., Cambridge University Press, 1997, pp. 88-102.

[2] Patriadi A., Soemitro R.A.A., Warnana D.D., Wardoyo W., Mukunoki T. and Tsujimoto G., The influence of Sembayat Weir on sediment transport rate in the estuary of BENGAWAN Solo River, Indonesia. International Journal of GEOMATE, Vol.20(81), 2021, pp. 35-43.

[3] Cenedese C., Nokes R. and Hyatt J., Lock-exchange gravity currents over rough bottoms. Environmental Fluid Mechanics, Vol. 18, 2018, pp. 59-73.

[4] Longo S., Ungarish M., Federico V. D., Chiapponi L. and Petroloa D., Gravity currents produced by lock-release: Theory and experiments concerning the effect of a free top in non-Boussinesq systems. Advances in Water Resources, Vol. 121, 2018, pp. 456-471.

[5] Beaird N. L., Shroyer E. L., Juranek L. W., Hales B. and Goñi M. A., Nutrient-Rich Gravity Current Formed by Upwelling in Barrow Canyon: High-Resolution Observations. Journal of Geophysical Research, Vol.125, Issue 7, 2020, e2020JC016160.

[6] Zhou M., Influence of Bottom Stress on the Two-layer Flow Induced by Gravity Currents in Estuaries. Estuarine, Coastal and Shelf Science, Vol. 46, Issue 6, 1998, pp. 811-825.

[7] Shin J. O., Dalziel S. B. and Linden P. F., Gravity currents produced by lock exchange. J. Fluid Mech, vol. 521, 2004, pp. 1-34.

[8] Dufek J. and Bergantz W., Suspended load and bed-load transport of particle-laden gravity currents: The role of particle-bed interaction. Theoretical and Computational Fluid Dynamics, Springer, Vol. 21(2), 2007, pp. 119-145.

[9] Traykovski P., Wiberg P.L. and Geyer W.R., Observations and modeling of wave-supported sediment gravity flows on the Po prodelta and comparison to prior observations from the Eel shelf. Continental Shelf Research, Vol.27, Issues 3-4, 2007, pp. 375-399.

[10] Nogueira H. I. S., Adduce C., Alves E. and Franca M. J., Analysis of lock-exchange gravity currents over smooth and rough beds. Journal of Hydraulic Research, Vol.51, Issue 4, 2013, pp. 417-431.

[11] Inghilesi R., Adduce C., Lombardi V., Roman F. and Armenio V., Axisymmetric three-dimensional gravity currents generated by lock exchange. J. Fluid Mech, vol. 851, 2018, pp. 507-544.

[12] Pelmard J., Norris S. and Friedrich H., Statistical characterisation of turbulence for an unsteady gravity current. J. Fluid Mech, Vol.901, 2020, pp. A7.

[13] De Falco M.C., Adduce C., Negretti M.E. and Hopfinger E.J., On the dynamics of quasi-steady gravity currents flowing up a slope. Advances in Water Resources, Vol.147, 2021, 103791.

[14] Maggi M.R., Adduce C. and Negretti M.E., Lock-release gravity currents propagating over roughness elements. Environ Fluid Mech, Vol.22, 2022, pp. 383-402.

[15] Sher D., Woods A. W., Gravity currents: entrainment, stratification and self-similarity. J. Fluid Mech, Vol.784, 2015, pp. 130-162.

[16] Baba N., Okamura S. and Fukuba T., Structure of head of gravity current. The Society of Naval Architects of Japan, Vol.184, 1998, pp. 197-205.